

Meanders

By GIOVANNI SEMINARA

Dipartimento di Ingegneria Ambientale, Università di Genova, Via Montallegro 1, 16145 Genova, Italy
sem@diam.unige.it

(Received 22 March 2005 and in revised form 7 December 2005)

In the last few decades cooperation among fluid dynamicists and geomorphologists has allowed the construction of a rational framework for the quantitative understanding of several geomorphologic processes involved in the shaping of the Earth's surface. Particular emphasis has been given to the dynamics of sedimentary patterns, features arising from the continuous dynamic interaction between the motion of a sediment-carrying fluid and an erodible boundary. It is this interaction which ultimately gives rise to the variety of natural forms, often displaying a high degree of regularity, observed in rivers, estuaries, coasts, as well as in the deep submarine environment. Theoretical analyses and laboratory experiments have shown that the nature of most of the observed patterns is related to fundamental instability mechanisms whose particular character lies in the fact that it is the mobile interface between the fluid and the erodible boundary, rather than the flow itself, that is unstable. Developments have been general enough to reach the status of a distinct branch of fluid mechanics, geomorphological fluid mechanics. This paper concentrates on the mechanics of fluvial meandering. Our aim is to provide the reader with a systematic overview of the fundamental aspects of the subject, assessing, with the help of recent and novel results, settled as well as unsettled issues.

1. Introduction

Twenty years ago a memorable special issue of this Journal was entirely devoted to the publication of the texts of lectures presented at the International IUTAM Symposium on *Fluid Mechanics in the Spirit of G. I. Taylor*, held at the University of Cambridge from 24 to 28 March 1986. One of the papers (Huppert 1986) had the inspiring title of 'The intrusion of fluid mechanics into geology'. The motivation was the recognition that geology offers a wide variety of fluid-mechanical phenomena in a distinct branch which Huppert named 'Geological Fluid Mechanics'. The present contribution is connected with that paper in that it shows that Huppert's prediction ('... There is every indication that the subject will continue to expand...') has indeed proved correct.

Here we are concerned with geomorphology, a branch of geology which investigates the variety of processes that shape the Earth's surface. The most important tools employed in this discipline are field observations coupled with the ability of geomorphologists to extract from the complexity of observations general behaviours describing how nature works. In the last few decades the scientific cooperation among a number of fluid dynamicists and geomorphologists has allowed the construction of a rational framework for the quantitative understanding of the origin and dynamics of sedimentary patterns, namely those features which develop as a result of the continuous dynamic interaction between the motion of a sediment-carrying fluid and

an erodible boundary: subaerial alluvial fans, rivers, estuaries, lagoons, coasts, deep submarine valleys are sedimentary environments displaying a rich variety of patterns shaped by the action of water. Theoretical analyses, as well as laboratory experiments, have clarified that the nature of most patterns is related to fundamental instability mechanisms whose particular character lies in the fact that it is the mobile interface between the fluid and the erodible boundary, rather than the flow itself, that is unstable.

Below, we restrict our attention to meandering, a pattern which offers a fascinating example of the ability that nature often displays to develop highly regular forms, a feature which has long attracted the interest of scientists and engineers (Einstein 1926). Meanders are ubiquitous in both sedimentary and non-sedimentary environments: they develop in sandy rivers wandering through flat valleys (figure 1*a*) as well as in narrow incisions constrained through rocky hill slopes or previously formed terraces (figures 1*b* and 1*c*). Meandering patterns form typically in sandy tidal channels as well as in vegetated cohesive salt marshes. Turbidity currents form gigantic meandering channels in submarine fans at the base of the continental slope (Imran, Parker & Pirmez 1999).

Our aim here is to provide the reader with a systematic overview of the fundamental aspects of the mechanics of fluvial meandering, assessing, with the help of recent and novel results, settled as well as unsettled issues. The subject matter is wide, hence we can only cover a few aspects, selected on the basis of our own research. The emphasis on our work should not be interpreted as an underestimation of the work of other groups, but rather as the need to follow a coherent line of thought we have developed since 1985 producing, we hope, a fairly complete rational framework for the understanding of the mechanics of meandering.

We start (§2) by outlining the main tools required to understand how meandering rivers evolve in space and in time: a nonlinear integro-differential planform evolution equation obtained by stipulating that the centreline of erodible channels moves in the lateral direction with some lateral migration speed, an erosion rule relating this erosion speed to the near-bank hydrodynamics and a model of flow and bed topography in sinuous channels required to predict near-bank flow. Next, we deal (§3) with the analysis of the mechanism (bend instability) whereby small perturbations of channel alignment of an initially straight channel may grow and develop a meandering pattern. Employing a linear model of flow and bed topography, we show that meanders behave as linear oscillators which may resonate at some distinct values of the aspect ratio of the channel and of the meander wavenumber. Resonance excites a natural mode of ‘oscillation’ of bed topography consisting of so called stationary alternate bars (see figure 5*a*): it turns out that crossing the resonance barrier leads to a reverse in directions of meander migration and of the dominant morphodynamic influence. The latter issue, i.e. the question of whether perturbations of channel morphology imposed at some cross-section of the river are dominantly felt downstream or upstream, is related to the nature of bend instability: this is found to be most often convective at a linear level with meander groups migrating downstream (upstream) under sub-resonant (super-resonant) conditions. This section is concluded with a brief discussion of the basic question of why meanders form in nature. In §4 we summarize the main features of the planform evolution of river meanders in the geometrically nonlinear regime: analytic periodic solutions of the evolution equation allow one to reproduce some very well-known field observations of mature meanders, namely their characteristic skewed shape, the temporal development of their lateral migration, the monotonic reduction of their migration speed which

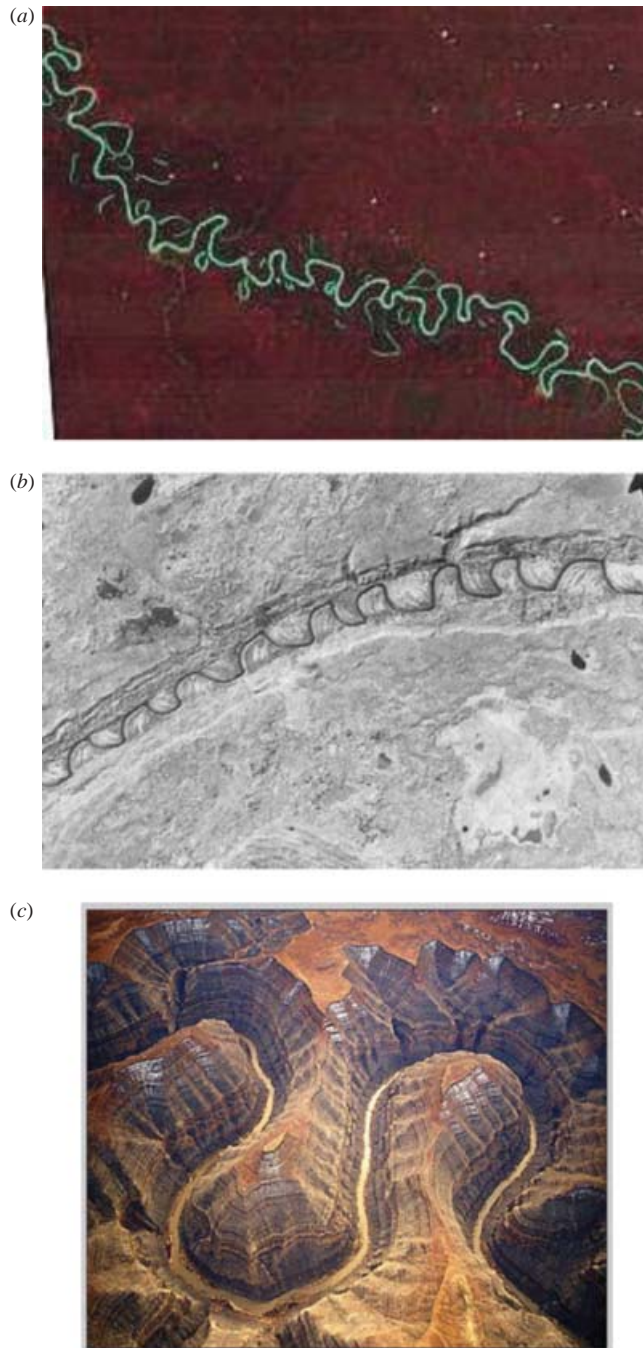


FIGURE 1. Examples of fluvial meandering patterns. (a) Meanders wandering in a flat valley (Brazilian Amazon): note several abandoned loops (oxbow lakes), multiple loops, upstream and downstream skewing. (b, c) Meanders constrained within narrow incisions bounded by rocky hillslopes: (b) Beaver river, Canada, from Allen (1984), (c) San Juan River, Goosenecks State Park, Utah, USA, photo copyright by Thomas Wiewandt www.wildhorizon.com.

nearly vanishes at neck cutoff (see figure 11). Numerical simulations starting from randomly perturbed straight configurations develop compound loops (see figure 1a) and confirm that bend instability most often (though not invariably) remains convective in the geometrically nonlinear regime. Section 5 is devoted to the effects of flow nonlinearities. We first recall some weakly nonlinear results able to predict the finite amplitude of near resonant meanders. We then move to the issue of whether alternate bars are able to ‘survive’, i.e. migrate, through meandering channels: field observations, suggesting that alternate bars are suppressed in ‘sufficiently curved’ channels, are interpreted by an early weakly nonlinear analysis, where free (migrating) bars (figure 5a) and forced (steady) bars (figure 11) are allowed to interact in a sequence of river bends. Finally, we attempt to explain the oscillations of channel width correlated with curvature often observed in meandering channels: a nonlinear perturbation solution able to account for flow nonlinearity is shown to achieve this goal. The interest of these results is enhanced by their possible implications for the as yet unresolved problem of predicting the occurrence of chute cutoffs (see figure 13a), a process whereby a meander can sometimes be abandoned well before neck cutoff. In fact, river widening is known to promote the formation of a central bar, hence a tendency to channel bifurcation: in a bend, this pattern is highly asymmetric (see figure 11), a feature which may lead to instability of the bifurcating flow and abandonment of the outer branch. Section 6 concludes the paper, emphasizing the need for further research and including warnings on the significance of planform simulations extended over geological time scales.

2. Formulation of the general problem of planform evolution of erodible channels

2.1. *Why does the planform shape of a meandering river evolve?*

Meandering rivers shift laterally and migrate longitudinally through a process of erosion (deposition) at concave (convex) banks. Erosion occurs continuously by removal of small particles from the bank surface and intermittently through bank collapse at the flood stage. This depends on a variety of factors (scour at the bank toe, bank cohesion, wetting and drying of banks, etc.) and its rate is ultimately controlled by the ability of the stream to remove sediments accumulated at the bank foot. This complex mechanism can be investigated in detail for single localized events. However, for long-term investigations, it is more appropriate to rely on an integrated description of the erosion process: in this approach, one essentially locates the region of the outer bank subject to erosion and replaces the actual intermittent process by an effective, spatially and temporally continuous, process reproducing the averaged effects of the former.

In the early development of the subject (e.g. Howard 1984; Howard & Knutson 1984) geomorphologists proposed kinematical models, where the lateral migration speed ζ^* (hereafter, a star denotes dimensional quantities) was empirically assigned. In the 1981 cornerstone paper of Ikeda, Parker & Sawai (which built upon a previous Japanese contribution) a dynamic approach was first proposed: bank erosion was assumed to be driven by an excess flow speed at the outer bank while bank deposition was conversely associated with a defect of flow speed at the inner bank. Hence, the erosion law is

$$\zeta = e(U|_{n=1} - U|_{n=-1}) \quad (2.1)$$

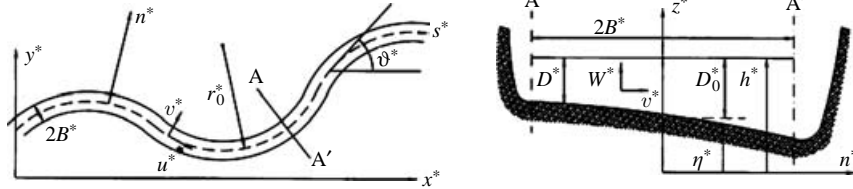


FIGURE 2. Sketch illustrating the planform evolution of meandering rivers and notation.

where both the lateral migration speed ζ^* and the depth-averaged longitudinal velocity U^* are scaled by some reference speed U_0^* , n is the lateral coordinate, with origin at the channel axis, scaled by half the channel width B^* , and e is a dimensionless long-term erosion coefficient. The suitability of the above linear rule has received some support (e.g. Pizzuto & Meckelnburg 1989) from field observations on rivers with fairly uniform cohesive banks. Moreover, (2.1) is conceived such that pure width variations do not affect the displacement of the channel centreline, hence channel width is preserved throughout the process of meander development.

Planform evolution equation

The problem of predicting the planform evolution of erodible channels then reduces to determining the motion of a line (the channel centreline) lying on a plane (a flat valley), such that each point of the line moves in the normal direction with the lateral migration speed ζ^* driven by bank erosion through the law (2.1). This motion is governed by a nonlinear partial integrodifferential equation which can be derived by purely geometrical arguments (Seminara, Tubino & Zardi (1994), Seminara *et al.* (2001)) and, in intrinsic dimensionless form, is

$$\vartheta_{,t} - \vartheta_{,t} \int_0^s \zeta \vartheta_{,s} ds = \zeta_{,s} \tag{2.2}$$

Here $\vartheta(s, t)$ is the angle that the local tangent to the channel axis forms with a Cartesian axis x^* (figure 2), with s the longitudinal coordinate and t time (respectively scaled by half the channel width B^* and by B^*/U_0^*). The form of (2.2) is readily understood by noting that a differential lateral migration of two adjacent points of the curve in a time interval dt (say $\zeta_{,s} ds dt$) drives a temporal variation of the angle ϑ associated with the material element ds . Evaluation of the latter requires noting that the instantaneous pattern (s, t) can be mapped into the initial pattern (s_0, t_0) through some relationship $s = s(s_0, t)$. Hence $\vartheta = \vartheta[s(s_0, t), t]$ and the derivative $d\vartheta/dt$ (left-hand side of (2.2)) involves an explicit as well as an implicit contribution. The latter contribution (second term on the left-hand side of (2.2), where the integral represents the material derivative ds/dt) accounts for the history of the channel deformation process. We have been recently made aware that the above problem has similarities with the general problem of interface evolution developed in the field of chemical physics (Brower *et al.* 1983, 1984). In order to close the formulation (2.1)–(2.2), a model for flow in sinuous erodible channels with arbitrary distribution of channel curvature is required.

2.2. Modelling flow and bed topography in sinuous channels

Research in the last three decades, stemming from the seminal papers of van Bendegom (1947), Rozovskij (1961) and Englund (1974), has clarified the physical ingredients of the process whereby flow and bed topography is established in a

sinuous channel (a wide perspective on the subject is found in Ikeda & Parker 1989). Let us briefly recall these ingredients. The lateral pressure gradient associated with a lateral slope of the free surface developing in a bend is unable to provide the centripetal force required to maintain the motion of fluid particles along curvilinear longitudinal trajectories: as a result, a secondary flow develops in the cross-section, directed outward close to the free surface and inward close to the bed. In fixed-bed bends, flow entering the bend is initially subject to a ‘free vortex’ effect whereby flow at the inner bend accelerates relative to the outer bend. Proceeding downstream, the secondary flow transfers momentum towards the outer bend, an effect which progressively prevails, moving the thread of high velocity from the inner to the outer bend. The cohesionless character of the bed further complicates the picture: secondary flow transports sediments in the lateral inward direction building up a rhythmic sequence of forced (point) bars and pools respectively at the inner and outer bends of a train of meanders. The establishment of a bar–pool pattern then gives rise to a further ‘topographically induced’ component of the secondary flow, which drives an additional contribution to sediment transport and further modifies the bed topography.

In order to place each of the contributions discussed below in the context of a unified framework, let us briefly outline the mathematical problem of flow and bed topography in sinuous cohesionless channels formulated in terms of the intrinsic coordinate system and of the dependent variables sketched in figure 2. We scale local mean velocity $(u^*, v^*, w^*)^T$, vertical coordinate z^* , flow depth D^* , free surface elevation h^* , bed elevation η^* , eddy viscosity ν_T^* and sediment flux per unit width $(q_s^*, q_n^*)^T$ as follows:

$$(z^*, D^*, \eta^*)^T = D_0^*(z, D, \eta)^T, \quad h^* = F_0^2 D_0^* h, \quad \nu_T^* = (\sqrt{C_{f0}} U_0^* D_0^*) \nu_T, \quad (2.3a-c)$$

$$(u^*, v^*)^T = U_0^*(u, v)^T, \quad w^* = \frac{U_0^*}{\beta} w, \quad (q_s^*, q_n^*)^T = \sqrt{(s_p - 1) g d^{*3}} (q_s, q_n)^T, \quad (2.3d-f)$$

where s_p is the relative particle density ($= \rho_s / \rho$ with ρ and ρ_s water and particle density respectively), d^* is particle diameter (taken to be uniform), C_{f0} is the friction coefficient, β is the aspect ratio of the channel, F_0 is the Froude number and the index 0 refers to the basic uniform flow associated with the average channel slope S . We define

$$\beta = B^* / D_0^*, \quad F_0^2 = U_0^{*2} / g D_0^*. \quad (2.4a, b)$$

Moreover, we take advantage of the fact that, in large scale river flow processes, the distribution of the mean pressure is hydrostatic. Using the definitions (2.3), (2.4), we can write the longitudinal and lateral components of the Reynolds equations, along with the continuity equations for the fluid and solid phases in dimensionless form. Assuming steady flow and a channel characterized by an arbitrary (yet slowly varying) spatial distribution of channel curvature $c(s)$ we find

$$h_s^{-1} u_{,s} + v_{,n} + w_{,z} = -h_s^{-1} \nu_0 c(s) v, \quad (2.5a)$$

$$h_s^{-1} u u_{,s} + v u_{,n} + w u_{,z} + h_s^{-1} h_{,s} - \beta \sqrt{C_{f0}} (\nu_T u_{,z})_{,z} = -h_s^{-1} [\beta C_{f0} + \nu_0 c(s) u v], \quad (2.5b)$$

$$h_s^{-1} u v_{,s} + v v_{,n} + w v_{,z} + h_{,n} - \beta \sqrt{C_{f0}} (\nu_T v_{,z})_{,z} = h_s^{-1} \nu_0 c(s) u^2, \quad (2.5c)$$

$$h_s^{-1} q_{s,s} + q_{n,n} = -h_s^{-1} \nu_0 c(s) q_n, \quad (2.5d)$$

where ν_0 is a curvature parameter defined in terms of some typical radius of curvature r_0^* and h_s is a metric coefficient, such that

$$\nu_0 = B^*/r_0^*, \quad h_s = [1 + \nu_0 c(s)]^{-1}. \quad (2.6a, b)$$

Equations (2.5) must be supplemented with classical kinematical and dynamic boundary conditions on the bottom and free surface, integral conditions for flow and sediment supply and closure relationships.

Providing a closure for the sediment flux would strictly require averaging its local and instantaneous value in time and space, a formidable task which is still beyond the present theoretical and computational capacities. Fortunately, for the purposes of morphodynamics, it is often sufficient to rely on a few fairly well-established results of semi-empirical nature which describe the motion of sediments in integrated form. Let us refer to the simplest flow conditions, namely uniform open channel flow over a homogeneous cohesionless plane bed (an equilibrium configuration by definition). Under these conditions, a few facts can be taken as fairly well-established.

(i) No significant sediment transport occurs below some critical value τ_{*c} of a dimensionless form τ_* (the Shields stress, Shields 1936) of the average shear stress τ acting on the bed: τ_{*c} is found to depend on the particle Reynolds number R_p . With ν_f the kinematic viscosity of the fluid, τ_* and R_p are

$$\tau_* = \frac{\tau}{(s_p - 1)gd^*}, \quad R_p = \frac{\sqrt{(s_p - 1)gd^{*3}}}{\nu_f}. \quad (2.7a, b)$$

(ii) For values of τ_* exceeding τ_{*c} but lower than a second threshold value τ_{*s} , particles are entrained, either individually or collectively, by the spatially and temporally intermittent generation of turbulent eruptions in the near-wall region (Drake *et al.* 1988). They then move close to the bed within a layer of thickness about a few grain diameters, saltating, rolling or sliding and eventually coming to rest to be entrained again after some time. In this type of sediment motion (bedload transport) particles have a distinct dynamics driven by, but different from, the dynamics of fluid particles. Under these conditions, the bed being flat (except for the possible presence of small scale bedforms), the average bedload flux per unit width \mathbf{q} is aligned with the uniform flow (i.e. with the direction of the average bottom stress $\boldsymbol{\tau}$) and its modulus (the bedload function Φ) is found to be a monotonically increasing function of the excess Shields stress ($\tau_* - \tau_{*c}$) for given particle Reynolds number R_p . A number of empirical or semi empirical relationships for Φ have been proposed in the literature (e.g. Meyer-Peter & Müller 1948).

However, large-scale morphodynamic features determine spatially slow perturbations of bed topography: on sloping beds, as a result of the gravitational tendency of particles to move downhill, bedload deviates from the direction of the local average bottom stress $\boldsymbol{\tau}$ by an amount which must be a function of the local value of the gradient of bed elevation. Assuming linearity, on purely dimensional grounds, deviation of the average bedload flux per unit width from the uniform behaviour is readily found to attain the general form

$$\mathbf{q} = \Phi(\tau_* - \tau_{*c}; R_p) \left(\frac{\boldsymbol{\tau}}{|\boldsymbol{\tau}|} + \mathbf{G} \cdot \nabla_h \eta \right), \quad (2.8)$$

where \mathbf{G} is a (2×2) matrix dependent on τ_* , τ_{*c} and on the angle of repose of the sediment. The elements of the matrix \mathbf{G} are also known semi-empirically. Note that relationship (2.8) generalizes ideas which go back to the early work of van Bendegom

(1947), later revisited by a number of further researchers. Also note that (2.8) fails close to sharp fronts (for the case of arbitrarily sloping beds, see Kovacs & Parker (1994) and Seminara, Solari & Parker (2003)).

When the local instantaneous value of the Shields stress exceeds a second threshold value τ_{*s} dependent on the particle Reynolds number, a second mode of sediment transport (in suspension), is observed to coexist with bedload transport. Particles, driven by near-wall ejection events, are collectively entrained by the flow and ‘nearly passively’ transported by the fluid in the outer region until they return to the bed under the effect of their excess weight. Below, space will force us to restrict our discussion to the case of bedload transport. The reader interested in the treatment of transport of dilute suspensions in open channels is referred to Bolla Pittaluga & Seminara (2003), where an analytic relationship for the depth-integrated suspended flux in slowly varying flows is derived.

Turbulent closures are not a prohibitive task in the case of river flow, which can often be treated as a slowly varying sequence of locally and instantaneously uniform flows. In several contexts, knowledge of the three-dimensional structure of the flow field is not even necessary and simpler, depth-averaged or one-dimensional formulations may be sufficient.

3. The nature of bend instability

Bend instability is the process whereby a perturbation of an initially straight channel alignment grows, driven by bank erosion, and leads eventually to the development of a meandering pattern. Employing a classical normal mode approach we consider the following perturbed state consisting of a sequence of so called sine-generated bends (Langbein & Leopold 1966):

$$\vartheta = \vartheta_1 \exp[i\lambda(s - at)] \quad (3.1)$$

with ϑ_1 the small initial amplitude of the perturbation, λ the intrinsic meander wavenumber scaled by $(B^*)^{-1}$ and a the complex wave speed scaled by U_0^* . In order to illustrate the mechanism of bend instability, it is instructive to examine first two simple examples.

3.1. Bank erosion in phase with curvature

Let us arbitrarily stipulate that the lateral migration speed ζ is proportional to and in phase with local curvature. Hence we set

$$\zeta = -\zeta_1 \vartheta_{,s}. \quad (3.2)$$

Substituting from (3.1), (3.2) into (2.1) and performing linearization, one finds an unsatisfactory picture of the process, namely meanders grow with a rate increasing indefinitely as the wavenumber increases and do not migrate:

$$\text{Re}(a) = 0, \quad \text{Im}(\lambda a) = \zeta_1 \lambda^2. \quad (3.3a, b)$$

3.2. Bank erosion out of phase relative to curvature

We now add an important ingredient, stipulating that the lateral migration speed ζ lags relative to local curvature by a length δB^* . Hence, we set

$$\zeta = -\zeta_1 \vartheta_{,s} \exp(-i\lambda\delta) \quad (3.4)$$

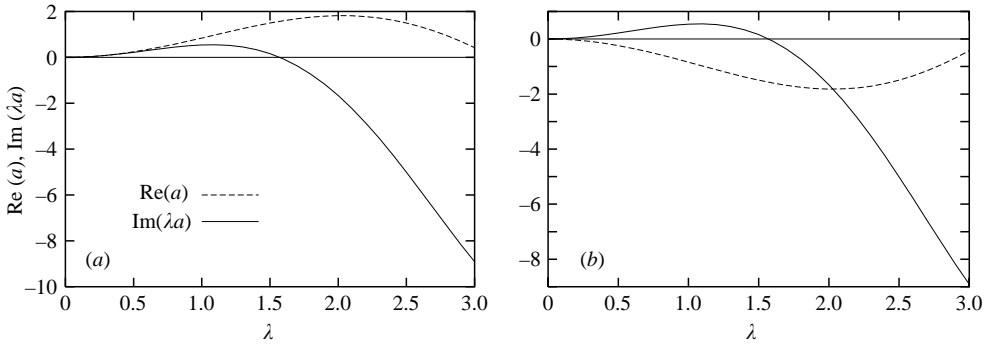


FIGURE 3. Dependence of growth rate and migration speed on meander wavenumber in the case of the erosion law (3.4) with (a) positive or (b) negative value of the phase lag δ between bank erosion and curvature. Both the amplitude ζ_1 and the modulus of the phase lag $|\delta|$ have been conventionally set equal to one.

to find

$$\text{Re}(a) = \zeta_1 \lambda \sin(\lambda\delta), \quad \text{Im}(\lambda a) = \zeta_1 \lambda^2 \cos(\lambda\delta). \quad (3.5a, b)$$

As shown in figure 3, under these conditions, meanders grow for values of meander wavenumber falling in the range $-\pi/2 < \lambda\delta < \pi/2$ and their growth rate shows a peak at some preferred wavenumber. In the same range, meanders migrate downstream if $\lambda\delta$ is positive, i.e. if the erosion peak is located downstream of the bend apex; conversely upstream migration is associated with negative values of $\lambda\delta$.

Though, in reality, the phase lag δ is not a constant but rather a function of meander wavenumber and of further relevant parameters, the picture offered by this simple example is quite close to the real one and illustrates the basic mechanism of meander growth and meander migration: the occurrence of a phase lag between flow perturbations (hence bank erosion) and curvature. The obvious next question is: what controls this phase lag? Answering this question requires sufficiently detailed knowledge of the flow field in sinuous erodible channels.

3.3. Linear solutions for flow and bed topography in sinuous channels

In Ikeda *et al.* (1981), a paper which has had a great influence on the subject, the hydrodynamics was described by the linearized shallow-water equations, while the conservation equations for the solid phase were not imposed and bed elevation was empirically assumed to increase linearly from the outer to the inner bank. Blondeaux & Seminara (1985) showed that decoupling hydrodynamics from bed topography implied that Ikeda *et al.*'s solution was only part of the complete solution of the problem. (This was later recognized by Johannesson & Parker (1989), who modified the approach of Ikeda *et al.* (1981) accordingly.) For a periodic sequence of small-amplitude sine-generated meanders (3.1) the complete linear solution of the problem is readily obtained by: (i) expressing it in the form $(u, v, w, h, D)^T \exp[i\lambda(s - at)]$, with λ the real meander wavenumber and a the complex wave speed; (ii) expanding $(u, v, w, h, D)^T$ in Fourier series in the n -direction as well as in powers of the typically small parameter ν_0 (Zolezzi & Seminara 2001); (iii) substituting from this expansion into the governing equations (2.5) with the closure (2.8) and with the further help of the erosion rule (2.1) and of the linearized form of the bend evolution equation (2.2). The following dispersion relationship for bend instability is eventually found

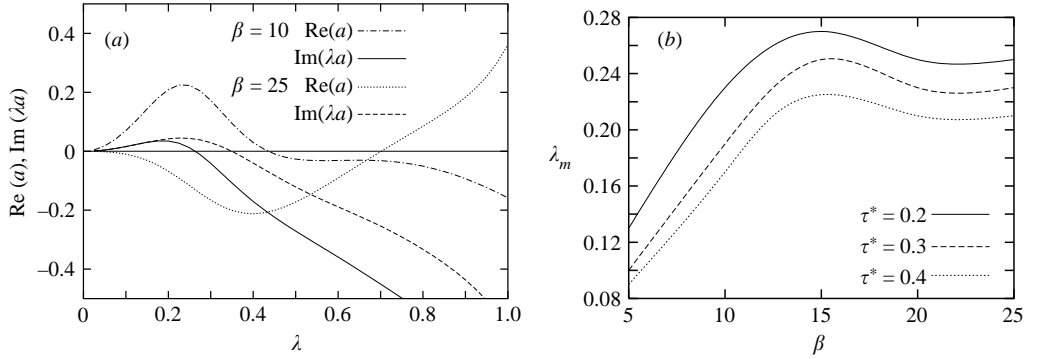


FIGURE 4. (a) Dependence of growth rate and migration speed on meander wavenumber under sub-resonant ($\beta = 10$) and super-resonant ($\beta = 25$) conditions ($\tau_* = 0.2$). (b) Dependence of the dimensionless wavenumber λ_m selected by bend instability on the aspect ratio β for a few values of the Shields stress τ_* . In both plots: $d^*/D_0 = 0.001$, the bed is dune covered.

(Seminara *et al.* 2001):

$$a = 2e \sum_{m=0}^{\infty} (-1)^{m+1} A_m \frac{\sum_{j=1}^7 \rho_j (i\lambda)^j}{\sum_{j=0} \sigma_j (i\lambda)^j} \quad (3.6)$$

where A_m is a coefficient (decreasing as m increases) quantifying the decaying contributions of higher lateral Fourier modes, while ρ_j and σ_j are functions of the parameters β , τ_* and C_{f0} . Figure 4, where (3.6) is plotted for realistic values of the latter parameters, shows that both the behaviours depicted in figure 3 may indeed characterize real meanders. In particular, a peak in the growth rate is observed at a value of the dimensionless wavenumber λ_m of about 0.1–0.3 (corresponding to wavelengths of about 30–10 channel widths respectively) (figure 4b). Moreover, the migration speed may indeed change sign (figure 4a). One would then like to know what mechanism controls the shift of the erosion peak from downstream to upstream of the bend apex.

3.4. Resonance and migration speed

The answer to the above question is only possible in the context of the solution of the coupled model: it turns out (Blondeaux & Seminara 1985) that linear meanders behave as linear oscillators which resonate at specific values λ_r and β_r of the meander wavenumber and of the aspect ratio of the channel, depending on the intensity of sediment transport (τ_*) and friction (C_{f0}). The functions $\lambda_r(\tau_*)$ and $\beta_r(\tau_*)$ are plotted in Seminara & Tubino 1992). In order to understand the physical origin of resonance, the reader should appreciate that a uniform turbulent free-surface flow on a cohesionless bed is naturally unstable to bottom perturbations, called free bars: sediment waves, of lengths scaling with channel width, arranged in alternate sequences of riffles and pools, a migrating pattern resembling the analogous, though steady, bar-pool pattern observed in meandering channels. Free bars may be arranged either in single rows (alternate bars), observed in sufficiently narrow channels (figure 5a) or in multiple rows (multiple row bars), observed in wide channels (figure 5b). The general characteristics of the free-bar instability have been thoroughly investigated (see the



FIGURE 5. Free bars: (a) alternate bars in the Rhine River, Switzerland (Jaeggi 1984); (b) multiple row bars in the Waimakariri (braided) River, New Zealand (courtesy of B. Federici).

review of Repetto, Tubino & Zolezzi 1999, and the recent contributions of Federici & Seminara (2003) and Hall (2004)). The marginal free modes are migrating modes at criticality (namely at critical values, λ_c and β_c , of the relevant parameters): however, along the marginal stability curve the migration speed varies and is found to vanish at the resonant values λ_r and β_r . At these conditions the free mode is stationary: while such a mode does not develop spontaneously, it can be excited in the presence of suitable forcing provided by channel curvature, leading to resonance.

A well-known feature of linear resonators (Kevorkian & Cole 1981, p. 141) is that the phase of the response changes quadrant on crossing the resonance conditions. In the meander case this feature implies that, on crossing resonance, the location of peak flow crosses the bend apex: note that this may be seen as a process occurring when the meander wavenumber λ increases for given aspect ratio β or, vice versa, when the aspect ratio β increases for given meander wavenumber λ . This has also been experimentally verified by Colombini *et al.* (1991) (figure 6) as well as by Garcia & Nino (1995). Recalling the erosion law (2.2) and the above discussion on the role of the phase lag between peak erosion and curvature, one immediately recognizes why sub-resonant (super-resonant) trains of periodic meanders migrate downstream (upstream) as found by Seminara *et al.* (2001).

3.5. Resonance and morphodynamic influence

The next step is to extend our knowledge on periodic meander trains to channels characterized by arbitrary distributions of channel curvature. One is then immediately faced with a fundamental question: are flow and bed topography at a given cross-section affected by the hydrodynamics and morphodynamics of the reach located upstream (downstream influence) or can the downstream reach also exert an influence (upstream influence)? Again the answer to this question is only possible in the context

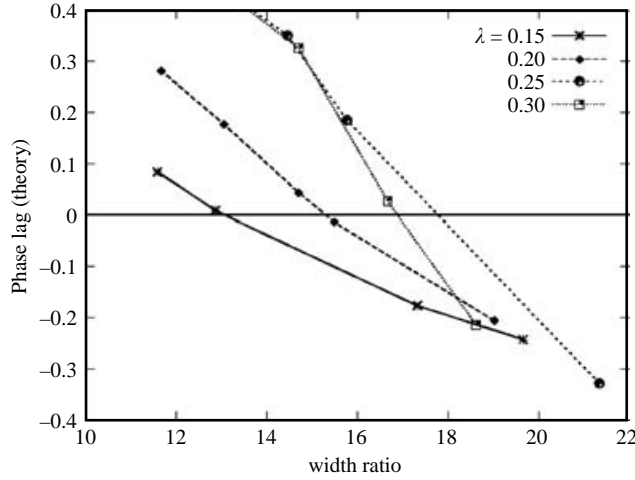


FIGURE 6. The phase lag ($\lambda\delta$) of the location of peak scour relative to the bend apex observed in a sine-generated bend is plotted as a function of the aspect ratio β of the channel for various meander wavenumbers λ (Colombini *et al.* 1991).

of a coupled model. In fact, using the uncoupled model of Ikeda *et al.* (1981), the erosion law (2.2) takes the form

$$\zeta = 2ev_0 \left[c(s) + \beta C_{f0} [(A_1 + 2)\chi + F_0^2 \chi^4] \int_0^s c(s - t) \exp(-2\chi\beta C_{f0}t) dt \right] \quad (3.7)$$

where χ is the ratio between the mean flow speeds in the sinuous and straight channels and A_1 is the amplitude of the lateral bed slope. It is apparent that (3.7) can only describe downstream influence; moreover, the latter decays without spatial oscillations over a length of the upstream reach affecting the local morphodynamics of a few hundred flow depths. The solution of Zolezzi & Seminara (2001) shows that the picture is less straightforward than suggested above, as two different scenarios occur under sub- and super-resonant conditions. For illustrative purposes, we show the form taken by the lateral migration rate when retaining only the first lateral mode in the solution:

$$\zeta = \Gamma_1 c(s) + g_1 \int_s^L \exp[-\lambda_1(t - s)]c(t) dt + g_2 \int_0^s \exp[-\lambda_2(s - t)]c(t) dt$$

$$+ g_3 \begin{cases} \int_0^s \exp[-\lambda_{3r}(s - t)] \cos[\lambda_{3i}(s - t) - \varphi]c(t) dt & \text{(sub-resonant)} & (3.8a) \\ \int_s^L \exp[\lambda_{3r}(s - t)] \cos[\lambda_{3i}(s - t) - \varphi]c(t) dt & \text{(super-resonant)} & (3.8b) \end{cases}$$

where Γ_i and $g_i (i = 1, 2, 3)$ are complicated functions of the parameters β, τ_* and C_{f0} while the characteristic exponents $\lambda_1, \lambda_2, \lambda_{3r}$ are real and positive and φ is the phase lag between erosion and curvature. Typically (Zolezzi & Seminara 2001), λ_1 and λ_2 are $O(1)$ quantities, implying a fast decaying influence, while λ_{3r} and λ_{3i} attain values of about 0.1, describing an influence which spreads over a considerable channel length. Various important features of (3.8) follow. In the sub-resonant case ($\beta < \beta_R$), the upstream distribution of channel curvature is felt downstream through the second and third convolution integrals of (3.8), with the former decaying fast upstream ($\lambda_2 \sim O(1)$) while the latter decays slowly ($\lambda_{3r} \ll 1$) and displays spatial oscillations;

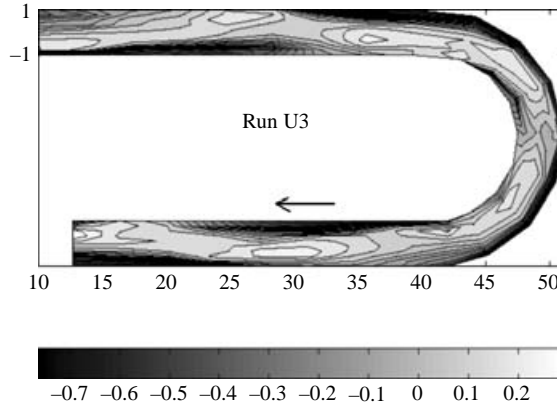


FIGURE 7. The pattern of bed topography observed in a 180° bend by Zolezzi *et al.* (2005) displaying the phenomenon of upstream influence whereby the presence of the bend is felt in the upstream reach through the formation of steady alternate bars.

the downstream distribution of channel curvature is felt only very weakly upstream through the first convolution integral which decays fast downstream ($\lambda_1 \sim O(1)$). The situation is reversed in the super-resonant case: the upstream distribution of channel curvature is felt weakly downstream through the second convolution integral of (3.8b); the downstream distribution of channel curvature is felt upstream through the first and third convolution integrals.

Note that both sub-resonant and super-resonant conditions are encountered in nature (see figure 7 of Zolezzi & Seminara 2001). Hence, seeking a field verification of the occurrence of upstream influence is an open challenge for geomorphologists. However, it is more feasible to pursue this goal through laboratory experiments. A successful attempt has been recently made by Zolezzi *et al.* (2005) who have monitored the bed pattern induced in 270° and 180° bends connected with upstream and/or downstream straight reaches. After filtering out the contribution to bed topography due to the effect of migrating free bars superimposed on the steady bar pattern developed at equilibrium, it turned out that, under super-resonant conditions a distinct steady bar does indeed form in the straight reach located upstream the bend. An example is given in figure 7 where upstream influence is also detected in the curved reach displaying a bar pattern which decays upstream.

3.6. The convective nature of bend instability

Let us complete our discussion on bend instability with an analysis of its fundamental nature: are we dealing with a convective or absolute type of instability?

We recall that instability is convective if an initial small perturbation is convected away (typically downstream) leaving, as time tends to infinity, the flow domain unperturbed. On the contrary, instability is absolute whenever the initial small perturbation spreads both in the upstream and downstream directions as time grows, eventually affecting the whole flow domain (e.g. Huerre & Monkewitz 1990). On investigating the response of the system to impulsive forcing, the nature of the instability turns out to depend on the occurrence of branch-point singularities in the dispersion relationship, i.e. values of ω ($\equiv \lambda a$ with a and λ both complex) where two or more spatial branches of the dispersion relationship merge. At branch-point singularities (ω_o, λ_o) the group velocity $[\partial\omega/\partial\lambda]_{\omega_o, \lambda_o}$ vanishes. A necessary condition for absolute instability is that the perturbation growth rate ω_i at the branch point must be positive; this condition is also sufficient provided at least two of the spatial

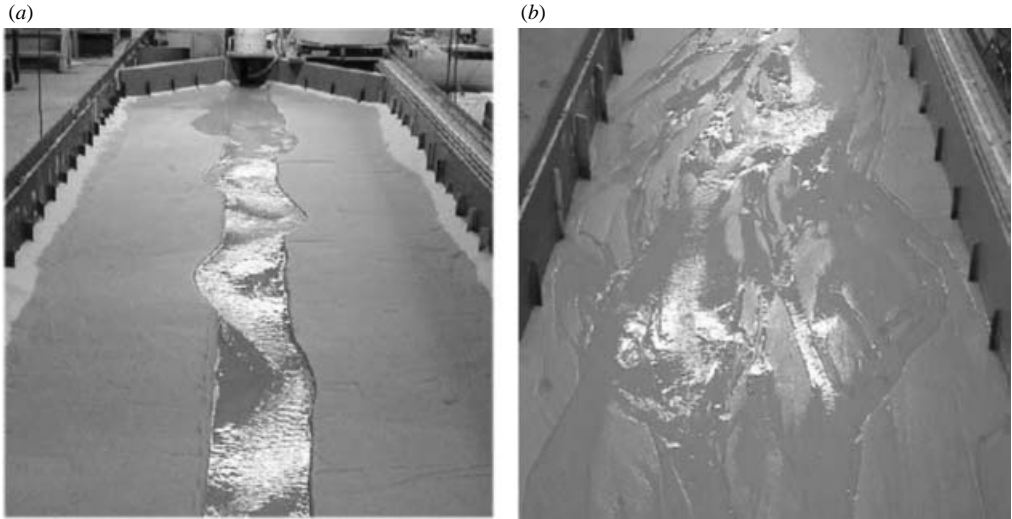


FIGURE 8. The laboratory experiment of Federici & Paola (2003) showing that the evolution of an initially straight channel cut through a cohesionless sediment layer eventually develops into a braided pattern; (a) $t = 15$ min, (b) $t = 20$ h.

branches of the dispersion relationship lie in distinct half- λ -planes for sufficiently large values of ω_i .

Application of such a criterion to bend instability (Lanzoni & Seminara 2006) suggests the existence of two typical scenarios. The first scenario arises when β is low enough: under such conditions, at a linear level, bend instability appears to remain invariably convective. The second scenario emerges for high values of β and is characterized by the existence of four complex branch points. Two of them, associated with the first Fourier mode, suggest a convective character of the instability; the remaining two singularities, associated with higher Fourier modes, suggest a transition to absolute instability for large values of β , a dune covered bed and large values of τ^* . In the absence of dunes a similar behaviour is observed, but for unrealistically high values of β . A further interesting feature emerges: the group velocity $[\partial\omega_r/\partial\lambda]_{\lambda_{\max}}$ (with λ_{\max} the wavenumber characterized by the maximum growth rate) changes sign as resonance is crossed: in other words, under super-resonant conditions the meander pattern propagates upstream.

3.7. *A basic yet academic question: why do meanders form?*

Bend instability theory predicts that any small random perturbation of channel alignment eventually grows, leading to a meandering pattern. Does this picture exhaustively answer the question of why meanders form and is it generally accepted?

Before embarking in a discussion of this problem, it is fair to say that the question of meander formation is somewhat academic because it is hard to substantiate any answer by field observations. On the other hand, rather surprisingly, laboratory observations have so far been unable to provide conclusive answers. In fact, cohesionless sediments are typically employed in these experiments: an initially straight incision through a flat layer of cohesionless material undergoes a sequence of processes (Federici & Paola 2003) associated with a continuous widening of the channel, driven by the erosion of cohesionless banks. Though, at an intermediate stage, an apparent meandering channel forms (figure 8a), it continues to evolve through further



FIGURE 9. The laboratory experiment of Gran & Paola (2001): in the run with the highest spatial vegetation density the river resembled a wandering stream, with one to two main channels separated by large, vegetated islands.

widening, the occurrence of chute cutoffs and the emergence of bars until a braided pattern, i.e. an interconnected network of channels, eventually develops (figure 8*b*). On the contrary, the persistence of a coherent meandering pattern requires a cohesive floodplain.

A recent successful attempt to reproduce this feature in the laboratory is due to Smith (1998). Gran & Paola (2001) performed an ingenious experiment on the related problem of braiding: they allowed a braided network to develop, then seeded the flume with alfaalfa (*Medicago sativa*), allowed the seeds to grow, and then continued the run. The influence of vegetation on overall river patterns was found to vary systematically with the spatial density of plant stems. As pointed out by the authors “In the run with the highest vegetation density, width to depth ratios approached those of natural single-thread channels. and in plan view the model resembled a wandering river, with one to two main channels flowing around larger vegetated islands [figure 9]. . . vegetation plays an important role in stabilizing the banks, constraining channel migration, and allowing deeper and narrower channels to develop. These are all effects that move the channel pattern in the direction of meandering”.

Geomorphologists have long speculated on alternate bars being precursors of river meandering (Leopold & Wolman 1957). However, this suggestion has various major shortcomings. First, alternate bars need to migrate fairly fast to be responsible for the localized erosion of cohesive banks driving meander formation. Secondly, and more importantly, the typical (dimensionless) wavenumber of developed alternate bars is about 0.5, hence it falls in the stable range of bend instability (recall figure 4). In other words, an alternate bar, seen as a planimetric perturbation of the channel axis, would not grow. Thirdly, alternate bars are observed to coexist with and migrate through weakly meandering channels (see § 5), an observation which contradicts the idea that they would evolve into the fixed-point bars of river meanders. Finally, in the experiments of Smith (1998) meandering developed in the absence of alternate bars and the chain of events typically observed (figure 5 of Smith 1998) did resemble

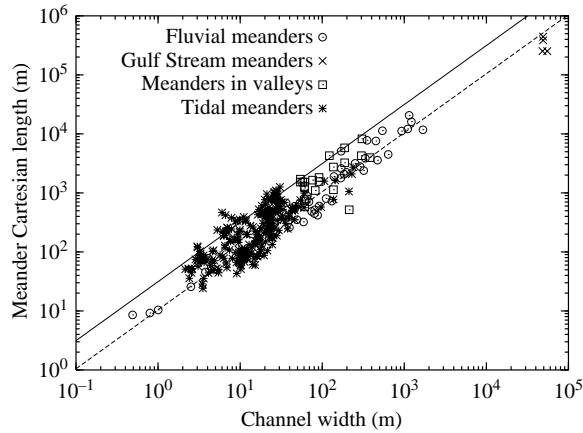


FIGURE 10. Correlation between Cartesian meander wavelength and channel width in various environments (from Marani *et al.* 2002).

the initial stage of a bend instability (figure 12 below). In conclusion, the ‘bend’ mechanism appears at this stage the only rational scheme able to explain various features observed in the field.

3.8. A related question: what is the relevant spatial scale of meanders?

As early as 1964 Leopold, Wolman & Miller proposed a celebrated diagram where the Cartesian length of meanders observed in vastly different environments was correlated with channel width. Figure 10 shows such a diagram enriched with further data referring to various tidal channels (Marani *et al.* 2002). Assuming that the preferred wavelength L_m is selected by the bend instability mechanism, theoretical results of figure 4(b) show that the dimensionless meander wavenumber ($\lambda_m = 2\pi B/L_m$) should fall in the range 0.1–0.3, depending on the values attained by the relevant physical parameters. Figure 10 shows that most experimental points do indeed fall within the predicted range.

Recently, Edwards & Smith (2002) have repeated some of the linear and nonlinear analyses previously developed by other authors, employing Ikeda *et al.*'s (1981) model (whose limits had already been known for nearly two decades). One of the statements of Edwards & Smith (2002) concerns the length scale of river meanders which they suggest, on dimensional grounds, coincides with the ratio between a typical flow depth and a typical friction coefficient of the flow: this length is the unique length over which the morphodynamic influence is felt in the context of Ikeda *et al.*'s model (see equation (3.7)). The above suggestion is not new: Parker & Johannesson (1989, p. 384) had already proposed rescaling the dimensionless meander wavenumber λ by the typically small quantity (βC_{f0}). However, the rescaled wavenumber (r in their notation) varied over more than two orders of magnitude in the 75 field cases they examined, a correlation worse than that obtained through the classical Leopold scaling. This is not surprising as Parker & Johannesson's rescaling is purely hydrodynamic: one may then reasonably wonder how it can account for meandering occurring in vastly different sedimentary environments. In the complete theory discussed above, the morphodynamic influence displays a more complex behaviour involving four spatial scales depending on the aspect ratio of the channel as well as on the intensity of sediment transport (τ_*) and friction (C_{f0}).



FIGURE 11. A meander bend close to neck cutoff showing that river width is a function of curvature and stage.

3.9. A real challenge for future research

A major open problem, which may concern some of the small meandering creeks observed in tidal marshes, as well as the astonishing fluvial patterns depicted in figure 1(c), is to understand the mechanics of meander formation in purely cohesive, erosional environments. In these cases, the classical bar–pool scheme must be abandoned in favour of a purely erosional mechanism driven by the three-dimensional structure of the flow field.

4. Planform evolution: effects of geometric nonlinearity

Let us next investigate the nonlinear planform evolution of river meanders: a number of field observations require theoretical explanations.

The first striking observation is that single meanders develop typically regular forms, described well by the fattened and skewed Kinoshita (1961) shape:

$$\vartheta = \vartheta_1 \exp(i\lambda s) + (\vartheta_{3r} + i\vartheta_{3i}) \exp(3i\lambda s) + \text{c.c.}, \quad (4.1)$$

fattening being associated with negative values of ϑ_{3r} and upstream (downstream) skewing with positive (negative) values of ϑ_{3i} . It is sometimes stated that one can infer from an aerial photo what is the flow direction of a meandering river, simply assuming that meanders are upstream skewed. This certainly applies to the regular meander train depicted in figure 1(b); less so for the river pattern of figure 1(a) where downstream and upstream skewing coexist and multiple loops are observed.

A second group of field observations concerns the temporal development of the growth rate and of the wave speed of meander trains: typically, the amplitude of single bends increases up to a peak and then decreases while their migration speed decreases monotonically (Nanson & Hickin 1983). Moreover, in the absence of geological constraints (like the confining valley walls of the Beaver river in figure 1(b), meanders typically (though not invariably) evolve continuously till neck cutoff (figure 11) occurs. This generates a geometric discontinuity of channel alignment which is smoothed out through further planform evolution: the abandoned loop (oxbow lake) is slowly filled up through the deposition of suspended sediments carried by overbank flows associated with floods. As the deposited sediments progressively consolidate,

the local valley erodibility changes slowly in time, a feature which may further affect the planform evolution on time scales of the order of centuries. Figure 1(a) shows clearly a number of neck cutoffs and oxbow lakes. A second type of cutoff (named chute cutoff, figure 13(a) below) may occur: in this case the loop is bypassed when the upstream and downstream branches are not yet close to neck cutoff. This process occurs in wide bends with fairly large curvatures, high discharges, poorly cohesive unvegetated banks and high slope (Howard & Knutson 1984).

Most of these observations have been explained by solving the fully nonlinear equation (2.1) coupled with a yet linear model for the flow field and bed topography.

4.1. Periodic meander trains

Let us first consider the periodic case. An analytical solution describing the nonlinear development of periodic sequences of meanders has been obtained by employing the following expansion for $\vartheta(s, t)$ (Seminara *et al.* 2001):

$$(\vartheta, \zeta) = \sum_{k=1}^{\infty} [\vartheta_k(t), \zeta_k(t)] \exp[i\lambda_k(t)s] + \text{c.c.} \quad (4.2)$$

where

$$\lambda_k = \frac{2\pi}{L(t)}(2k - 1) = (2k - 1)\lambda(t) \quad (4.3)$$

with $L(t)$ meander wavelength. Note that: (i) (4.2), (4.3) is not a classical Fourier expansion for $\vartheta(s, t)$ as the wavenumber of each Fourier mode here is allowed to vary in time; (ii) even harmonics are absent as a consequence of the cubic nonlinearity of the evolution equation (2.1); (iii) retaining only the first term of the expansion, one recovers the sine-generated shape of Langbein & Leopold (1966) while, on retaining the first two terms, Kinoshita's (1961) shape is found: hence, the patterns emerging from observations of geomorphologists are not purely empirical correlations, but rather different approximations of an exact periodic solution of the planform evolution equation.

Substituting from the above expansion into the evolution equation (2.1) and equating terms proportional to $\exp(i\lambda_k s)$ ($k=0, 1, 2, \dots, N$) one ends up with a coupled system of N nonlinear ordinary differential equations for the amplitudes $\vartheta_k(t)$ ($k=1, 2, \dots, N$) plus an equation for the meander wavenumber $\lambda(t)$. The solution of this system exhibits features in accordance with field observations. In particular: (i) spatial harmonics higher than the third do not play a significant role as neck cutoff typically occurs before they have a chance to amplify, as suggested by Kinoshita's observations; (ii) the monotonic reduction of the migration speed of natural meanders which tends to vanish prior to cutoff as well as the non-monotonic behaviour of the lateral migration of meander trains is reproduced; (iii) downstream (upstream) migration and upstream (downstream) skewing of meander patterns is obtained under sub-resonant (super-resonant) conditions (figure 11), a feature associated with a variation of the phase of the third harmonics relative to the fundamental (Seminara *et al.* 2001); (iv) compound loops form in the super-resonant case prior to neck cutoff as a consequence of the faster amplification of higher harmonics; (v) the existence of meanders of permanent form migrating in the longitudinal direction with no growth or decay in the absence of geological constraints is unlikely, but has not been conclusively excluded. However, provided the dominant contribution to meander shape arises from the fundamental sine-generated component of curvature,

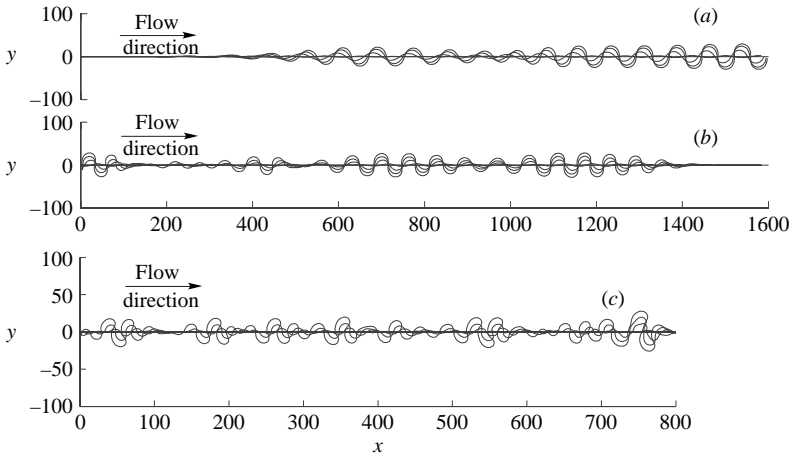


FIGURE 12. The nonlinear response to bend instability: wave groups develop and migrate downstream (upstream) under sub-resonant (super-resonant) conditions. (a) $\beta = 22$, $\tau_* = 0.20$, $d^*/D_0^* = 0.004$, flat bed, $e = 2 \times 10^{-8}$: instability is convective; (b) $\beta = 30$, $\tau_* = 0.1$, $d^*/D_0^* = 0.01$, flat bed, $e = 2 \times 10^{-8}$: instability is convective; (c) $\beta = 25$, $\vartheta = 0.7$, $d_S = 0.005$, dune covered bed, $e = 1.85 \times 10^{-8}$: instability is absolute (Lanzoni & Seminara 2006).

no equilibrium solution is possible. Note that a periodic solution of permanent form was found by Parker, Diplas & Akiyama (1983) and later shown to be unstable by Parker & Andrews (1986).

4.2. The convective nature of bend instability in the nonlinear regime

In §3 we have shown that linear bend instability is convective except in the highly super-resonant regime. In order to ascertain whether such a behaviour persists in the (at least geometrically) nonlinear regime, Lanzoni & Seminara (2006) have solved the planform evolution equation numerically, starting from a straight configuration of the channel axis which is then slightly and randomly perturbed. No constraint was imposed at the end cross-sections: in other words, the planform was allowed to evolve freely. The complete solution for flow and bed topography of Zolezzi & Seminara (2001) was employed and both the sub-resonant and the super-resonant scenarios were examined. The initial stage of the nonlinear response is shown in figure 12, which confirms the existence of the two scenarios that emerged in the linear case: when β is low enough bend instability is convective (figure 12a, b); for large values of β , dune covered beds and large values of τ_* , a transition to absolute instability is found (figure 12c). Furthermore, the group velocity changes sign as resonance is crossed: in other words, under super-resonant conditions the meander pattern propagates upstream. We do not yet know whether this is a general feature of the instability of forced resonating systems. However, the physical implications of these findings is notable: in super-resonant meanders morphodynamic information propagates upstream. This appears to be a significant theoretical achievement which calls for some conclusive field verification: an example of upstream migration, kindly provided by W. Dietrich, is reported in Seminara *et al.* (2001).

Note that, in the context of the uncoupled model of Ikeda *et al.* (1981) bend instability is also convective but wave groups can only migrate downstream.

5. The effects of flow nonlinearity

We now examine some physically important processes controlled by flow nonlinearity, starting with a short description of early results and then outlining some novel results.

5.1. Weakly nonlinear near-resonant meanders

The first question deserving attention is to ascertain the nonlinear behaviour of near-resonant meanders: Seminara & Tubino (1992) then sought the finite-amplitude flow and bed topography developing in periodic sequences of sine-generated meanders, characterized by values of the wavenumber λ and aspect ratio β close to their resonant values, λ_R and β_R respectively. The solution for flow and bed topography in a neighbourhood of resonance was expanded in powers of the small curvature ratio v_0 as follows:

$$\beta = \beta_R + v_0^{2/3} \beta_I, \quad \lambda = \lambda_R + v_0^{2/3} \lambda_I, \quad (5.1a, b)$$

$$\begin{aligned} U = & 1 + v_0^{1/3} [A \sin(\pi n/2) \exp(i\lambda_R s)] \\ & + v_0^{2/3} [A^2 (U_{20} + U_{22} \cos(\pi n)) \exp(2i\lambda_R s) + A\bar{A} (U_{00} + U_{02} \cos(\pi n))] \\ & + v_0 [A_{31} \sin(\pi n/2) \exp(i\lambda_R s)] + \text{c.c.} + \text{higher harmonics.} \end{aligned} \quad (5.2)$$

Note that the leading-order component of (5.2) is the resonating stationary bar mode mentioned in §3; also, note that its amplitude is much larger ($O(v_0^{1/3})$) than that of the linear non-resonant solution ($O(v_0)$). Substituting from the expansion (5.1), (5.2) (and similar expansions for V , h , D) into the depth-averaged form of the conservation equations and following the classical perturbation approach, at third order secular terms are obtained whose suppression leads to deriving a nonlinear cubic algebraic equation for the complex amplitude A with coefficients dependent on β_I and λ_I . Its solution displays characteristics typical of weakly nonlinear resonators, namely nonlinear damping and non-uniqueness of the response (Kevorkian & Cole 1981). Moreover, nonlinearity increases the meander wavenumber at which the flow response peaks. The above results have received some experimental support (Colombini *et al.* 1991).

5.2. nonlinear interaction between free and forced bars

A second fundamental observation is due to Kinoshita & Miwa (1974): free migrating bars, which are known to form in straight channels (figure 5a) are suppressed in sufficiently sinuous channels, i.e. when forced bars are also present. The analysis of Tubino & Seminara (1990) shows that the suppression mechanism is a sort of destructive interference between steady and migrating modes. The basic idea was to allow for the interaction of free and forced bars in a weakly nonlinear context. At the leading order of approximation, any property of a free alternate bar (say its velocity) close to critical conditions may be represented in the form

$$U = \epsilon^{1/2} A \sin(\pi n/2) \exp[i(\lambda_c s - \omega t)], \quad (5.3)$$

where the small parameter ϵ equals $[(\beta - \beta_c)/\beta_c]$, with β_c critical value of the aspect ratio of the channel, λ_c the critical wavenumber and ω the complex growth rate (Colombini *et al.* 1987). Similarly, at the leading order of approximation, the velocity of forced bars in a sine-generated meander, is

$$U = v_0 [u(n) \exp(i\lambda_m s)], \quad (5.4)$$

with λ_m the meander wavenumber. We now stipulate that curvature (i.e. v_0) is large enough for the amplitude of forced bars to be comparable with the amplitude of free bars and set

$$v_0 = k \sqrt{\frac{\beta - \beta_c}{\beta_c}}, \quad (5.5)$$

with k an $O(1)$ parameter to be determined. We then let the migrating mode (5.3) interact with the steady mode (5.4). At $O(\epsilon v_0)$ nonlinear interactions reproduce the fundamental alternate bar mode leading to the generation of secular terms whose suppression allows us to determine the threshold value of k for the suppression of free bars as a function of meander wavenumber. Results agree fairly well with the laboratory observations of Kinoshita & Miwa (1974).

The coexistence of free and forced bars has various practical implications: in particular, restoration work aimed at stabilizing the bed of rivers can use to advantage the suppression of migrating features obtained by choosing a slightly sinuous alignment for the restored channel.

5.3. A further consequence of flow nonlinearity: spatial oscillations of river width

The next basic question to be examined concerns the width of meandering rivers. Figure 11 motivates such an investigation, showing that the width of the stream free surface may undergo spatial oscillations correlated with channel curvature.

This observation is not universally true: so-called canaliform rivers flowing in highly vegetated flood plains may exhibit an opposite behaviour. Solari & Seminara (2005) have recently attempted to explain the above observations.

Physically, the idea is straightforward. As sediment transport is nonlinearly related to flow velocity, in order to allow a constant flux of sediment and a constant discharge through a sinuous channel, the channel width must necessarily vary. In order to implement this idea Solari & Seminara (2005) extend their previous work (Seminara & Solari 1998) on finite-amplitude bed deformations in constant-curvature channels with constant width. Flow and bottom topography are assumed ‘slowly varying’ in both longitudinal and lateral directions while curvature effects (hence v_0) are taken to be ‘small’: the former assumption essentially requires the channel to be ‘wide’ with width and channel alignment varying on a longitudinal scale much larger than channel width. Both conditions are indeed satisfied in actual rivers but, in spite of the popularity enjoyed by linear models, neither of them implies that perturbations of bottom topography are necessarily small. The analytical approach of Solari & Seminara (2005) successfully removes this restriction; channel width B^* is taken to oscillate around some average value B_u^* , and the coordinates s , n and ζ are rescaled as follows:

$$\sigma = \frac{s^*}{r_0^*} = v_0 s, \quad B^* = B_u^* b(\sigma), \quad y = \frac{n^*}{B^*} = \frac{n^* B_u^*}{B_u^* B^*} = \frac{n}{b(\sigma)}, \quad Z = 1 + \frac{z - h(y, \sigma)}{D(y, \sigma)}, \quad (5.6a-d)$$

with $b(\sigma)$ unknown ‘slowly varying’ function to be determined.

The solution is then expanded in a neighbourhood of the solution for uniform flow in a straight channel with unknown slowly varying shape of the bottom profile described by a function $D(y, \sigma)$ which, along with the function $b(\sigma)$, is the major output of the analysis. The appropriate extension of Seminara & Solari’s (1998)

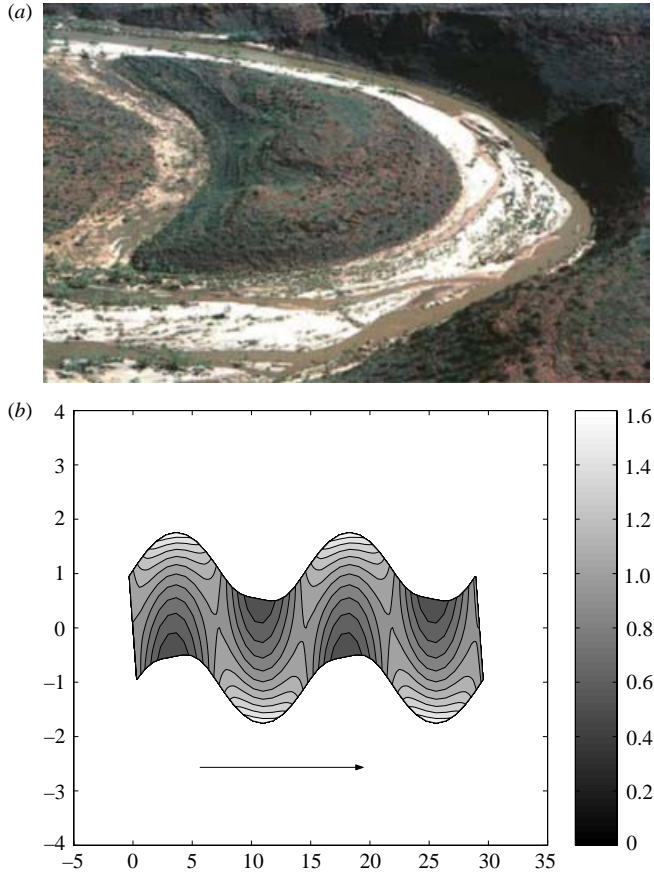


FIGURE 13. (a) A paleomeander showing a chute cutoff and the formation of a central bar close to the bend apex (Finke river, Australia, courtesy of Aberdeen University, Geoff Pickup). (b) Characteristic channel widening generated by the theory of Solari & Seminara (2006) for a sequence of short sine-generated meanders ($\tau_* = 0.15$, $d^*/D_0^* = 0.01$, $\lambda = 0.419$).

expansion is

$$(u, v, w, h, D, b)^T = [u_0(Z; y, \sigma), 0, 0, 1, D_0(y, \sigma), b_0(\sigma)]^T + \sum_{m=1}^{\infty} \left(u_m, v_m, \frac{w_m}{\beta_u}, h_m, D_m, b_m \right)^T \epsilon^m \quad (5.7)$$

where ϵ is the small parameter $v_0/\beta_u \sqrt{C_{fu}}$. Substituting from (5.7) into the governing differential problem (2.5), rewritten in terms of the transformed variables σ, y and ζ and equating likewise powers of ϵ , one obtains a sequence of differential problems, readily solved in terms of the unknown functions D and b . Reinforcing integral constraints whereby flow and sediment discharges must keep constant in the longitudinal direction leads to nonlinear partial differential equations at various orders whose solutions allow one to determine the functions $b(\sigma)$ and $D(y, \sigma)$ by a trial and error procedure.

A sample of results obtained by Solari & Seminara (2005) is reported in figure 13(b), where a sequence of fairly short meanders displays the characteristic widening of the cross-section observed close to the bend apex on the side of the point bar (figure 11).

Recent developments (Solari *et al.* 2006) suggest that the above picture changes as the Shields stress increases: narrowing of the cross-section is predicted at the bead apex and multiple solutions arise.

Figure 13(a) shows the formation of an island in a meandering channel close to the bend apex: it is natural to wonder whether the mechanism underlying the formation of a central stationary bar may be related to a bottom instability driven by width variations of a curved channel. A further significant speculation will require attention: the formation of a central bar at the apex is likely to promote a tendency of the stream to bifurcate into an outer and an inner branch, the latter being a potential precursor of chute cutoff (Jager 2003).

6. Beyond cutoff: patterns on the geological time scale

The investigations discussed above concerned meandering processes occurring on small or moderate time scales. A number of geomorphologists have employed models of planform evolution in order to simulate processes occurring on geological time scales. In particular, Sun *et al.* (1996) investigated the formation of meander belts (Jefferson 1902), i.e. the confinement of the evolving river pattern to a restricted portion of the floodplain. The simulations were based on Ikeda *et al.*'s model, modified to account for the increased erodibility of the floodplain in areas formerly occupied by point bars and the decreased erodibility of areas occupied by oxbow lakes. The formation of a belt was found to depend on how fast the process of filling of the oxbow lakes is relative to the time scale of river migration over a meander wavelength. The evolution of flood plains was simulated by Howard (1996) coupling Johannesson & Parker's (1989) model for planform evolution with a lattice model for the floodplain accounting for overbank sedimentation through an empirically simulated deposition rate. The fashionable, yet delicate, issue of predictability of meander evolution has also been tackled on the basis of the analysis of sequences of patterns produced through numerical simulations (Stolum 1996): they suggest that the occurrence of neck cutoffs is the cause of an intermittently chaotic behaviour of meandering patterns.

A few words of caution on the suitability of models employed in various simulations may be appropriate at this stage. As pointed out by Howard (1996), the planform shapes generated by simulations based on Johannesson & Parker's (1989) model are characterized by sinuosities (the ratio between intrinsic and Cartesian meander lengths) significantly higher than those typically observed in nature. This limitation does not seem to be present in simulations based on the complete hydrodynamic model. This is shown in figure 14, where the planform evolution is carried on beyond cutoff: the average sinuosity of the river reach shows an oscillatory damped behaviour tending to nearly constant values quite representative of actual meandering patterns.

Also, one may reasonably wonder whether the relative simplicity of the tools employed is appropriate to account for the complexity of the events which shape the real system. Let us then make some concluding remarks on this issue.

The stochastic nature of the physical characteristics of our system has been ignored: in particular, bank erodibility depends on the previous history of the planform evolution process, as well as on the presence of vegetation, geological constraints and anthropogenic effects.

The flow is assumed to be steady: the discharge as well as channel width, river slope and grain size are taken to be constant. These assumptions are acceptable when the spatial scale of the reach as well as the temporal scale of the process are not too large.

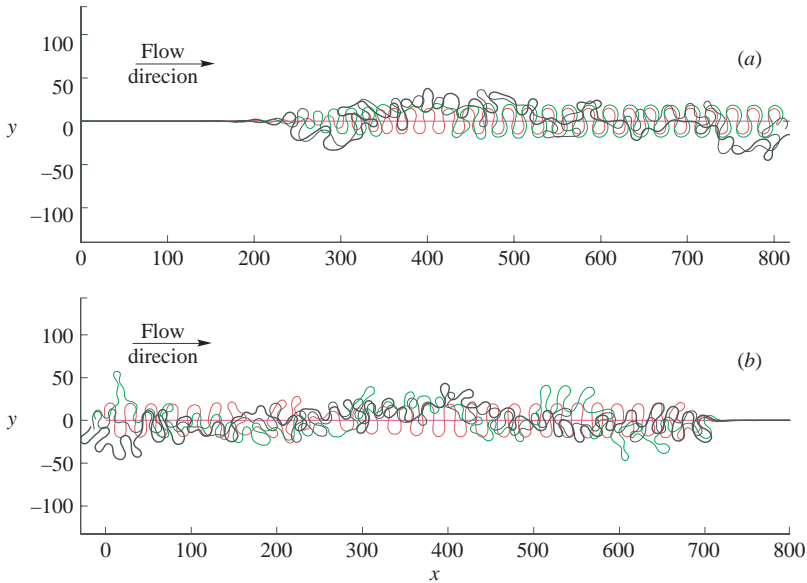


FIGURE 14. Numerical simulations beyond cutoff: (a) sub-resonant case, $\beta = 9$, $\tau_* = 0.3$, $d_s = 0.005$, $E = 10^{-8}$, dune covered bed; (b) super-resonant case, $\beta = 13$, $\tau_* = 0.3$, $d_s = 0.005$, $E = 10^{-8}$, dune-covered bed. Note the formation of compound loops. Also note that sinuosity decreases as development proceeds. In the sub-resonant case: red 2.67; green 3.08; black thin 1.80; black thick 1.69. In the super-resonant case: red 2.98; green 2.22; black thin 2.32; black thick 2.45. (Calculations kindly provided by S. Lanzoni, 2005).

At larger scales, spatial variations of discharge and the presence of tributaries impose significant constraints while the effects of grain sorting are likely to be not negligible.

Sediment transport is invariably assumed to be bedload dominated, though suspension is the dominant form of transport in sandy streams at the formative stage. Moreover, chute cutoffs are not simulated and the way neck cutoff is modelled is quite schematic: in particular the process of river degradation – aggradation driven by the cutoffs is ignored, though its spatial and temporal scales may be large enough to play some role in the further planform evolution of the adjacent river reach.

The end conditions are often set arbitrarily and are not always compatible with the actual nature of bend instability. Finally, flow nonlinearity is not accounted for.

One needs be aware of the above limits when judging results of the investigations discussed above. The soundness of the theoretical treatment of relatively small-scale processes has often been substantiated (at least qualitatively) through field or laboratory observations. This is the ultimate criterion allowing us to distinguish between scientific investigations, able to improve our knowledge of the physical system, and possibly complex mathematical exercises which may sometimes reduce to enjoyable computer games. It is with this qualification that the cross-fertilizing interaction between scientists belonging to different communities, who often bring fresh viewpoints (e.g. Liverpool & Edwards 1995), must be encouraged and strongly welcomed.

This paper is dedicated to a special person, my wife: marrying a scientist and persisting so long is a burden which deserves to be warmly acknowledged. I also wish to thank my former students and present coworkers S. Lanzoni, B. Federici

and L. Solari for allowing me to report results of some joint, as yet unpublished, works. Funding from MIUR and from the University of Genova (PRIN 2003, “Idromorfodinamica fluviale e interazioni con manufatti e processi naturali”) is gratefully acknowledged. Partial support has also come from Fondazione CARIVERONA.

REFERENCES

- ALLEN, J. R. L. 1984 *Sedimentary Structures*. Elsevier.
- VAN BENDEGOM, L. 1947 Some consideration on river morphology and river training. *De Ingenieur* **59**(4), B1–B12.
- BLONDEAUX, P. & SEMINARA, G. 1985 A unified bar-bend theory of river meanders. *J. Fluid Mech.* **112**, 363–377.
- BOLLA PITTALUGA, M. & SEMINARA, G. 2003 Depth-integrated modeling of suspended sediment transport. *Water Resour. Res.* **39**, ESG1, 1–13.
- BROWER, R. C., KESSLER, D. A., KOPLIK, J. & LEVINE, H. 1983 Geometrical approach to moving-interface dynamics. *Phys. Rev. Lett.* **51**, 1111–1114.
- BROWER, R. C., KESSLER, D. A., KOPLIK, J. & LEVINE, H. 1984 Geometrical models of interface evolution. *Phys. Rev. A* **29**, 1335–1342.
- COLOMBINI, M., SEMINARA, G. & TUBINO, M. 1987 Finite-amplitude alternate bars. *J. Fluid Mech.* **181**, 213–232.
- COLOMBINI, M., TUBINO, M. & WHITING, P. 1991 Topographic expression of bars in meandering channels. In *Dynamics of Gravel-bed Rivers* (ed. P. Billi, R. D. Hey, C. R. Thorne & P. Tacconi). John Wiley and Sons.
- DRAKE, T. G., SHREVE, R. L., DIRTRICH, W. E., WHITING, P. J. & LEOPOLD, L. B. 1988 Bedload transport of fine gravel observed by motion picture. *J. Fluid. Mech.* **192**, 193–217.
- EDWARDS, B. F. & SMITH, D. H. 2002 River meandering dynamics. *Phys. Rev. E* **65**, 046303.
- EINSTEIN, A. 1926 Die Ursache der Mäanderbildung der Flußläufe und des sogenannten Baerschen Gesetzes. *Die Naturwissenschaften* **11**, 223–224.
- ENGELUND, F. 1974 Flow and bed topography in channel bends. *J. Hydr. Div. ASCE* **100**, 1631–1648.
- FEDERICI, B. & PAOLA, C. 2003 Dynamics of channel bifurcations in non cohesive sediments. *Water Resour. Res.* **39**, ESG3, 1–15.
- FEDERICI, B. & SEMINARA, G. 2003. On the convective nature of bar instability. *J. Fluid Mech.* **487**, 125–145.
- GARCIA, M. & NINO, Y. 1995 Dynamics of sediment bars in straight and meandering channels: experiments of the resonance phenomenon. *J. Hydr. Res.* **31**, 739–761.
- GRAN, K. & PAOLA, C. 2001 Riparian vegetation controls on braided stream dynamics. *Water Resour. Res.* **37**, 3275–3283.
- HALL, P. 2004 Alternating bar instabilities in unsteady channel flows over erodible beds. *J. Fluid Mech.* **499**, 49–73.
- HOWARD, A. D. 1996 Modelling channel evolution and floodplain morphology. In *Floodplain Processes* (ed. M. G. Anderson, D. E. Walling & P. D. Bates), pp. 15–62. John Wiley & Sons.
- HOWARD, A. D. & KNUTSON, T. R. 1984 Sufficient conditions for river meandering: a simulation approach. *Water Resour. Res.* **20**, 1659–1667.
- HUERRE, P. & MONKEWITZ, P. A. 1990 Local and global instabilities in spatially developing flows. *Annu. Rev. Fluid Mech.* **22**, 473–537.
- HUPPERT, H. 1986 The intrusion of fluid mechanics into geology. *J. Fluid Mech.* **173**, 557–594.
- IKEDA, S. & PARKER, G. (Eds.) 1989 *River Meandering*. Water Res. Monograph 12, AGU.
- IKEDA, S., PARKER, G. & SAWAI, K. 1981 Bend theory of river meanders. Part 1. Linear development. *J. Fluid Mech.* **112**, 363–377.
- IMRAN, J., PARKER, G. & PIRMEZ, C. 1999 A nonlinear model of flow in meandering submarine and subaerial channels. *J. Fluid Mech.* **400**, 295–331.
- JAEGGI, M. N. R. 1984 Formation and effects of alternate bars. *J. Hydr. Div. ASCE* **110**, 142–156.
- JAGER, H. R. A. 2003 Modelling planform changes of braided rivers. PhD Thesis, University of Twente.
- JEFFERSON, W. S. 1902 Limiting width of meander belts. *Natl Geogr. Mag.* **13**, 373–383.

- JOHANNESSON, H. & PARKER, G. 1989 Linear theory of river meanders. In *River Meandering* (ed. S. Ikeda & G. Parker). Water Res. Monograph 12, pp. 181–214. AGU.
- KEVORKIAN, J. & COLE, J. D. 1981 *Perturbation Methods in Applied Mathematics*. Springer.
- KINOSHITA, R. 1961 An investigation of channel deformation of the Ishikari River. *Tech. Rep.*, Natural Resources Division, Ministry of Science and Technology of Japan.
- KINOSHITA, R. & MIWA, H. 1974 River channel formation which prevents downstream translation of transverse bars. *Shinsabo* **94**, 12–17, in Japanese.
- KOVACS, A. & PARKER, G. 1994 A new vectorial bedload formulation and its application to the time evolution of straight river channels. *J. Fluid Mech.* **267**, 153–183.
- LANGBEIN, W. B. & LEOPOLD, L. B. 1966 River meanders – Theory of minimum variance. *US Geol. Surv., Prof. Paper* 422-H, Hi-H15.
- LANZONI, S. & SEMINARA, G. 2006 On the convective nature of bend instability. *J. Geophys. Res.* (submitted).
- LEOPOLD, L. B. & WOLMAN, M. G. 1957 River channel patterns, braided, meandering and straight. *US Geol. Survey, Prof. Paper* 282-B, pp. 45–62. Reproduced in *Rivers Morphology* (ed. S. A. Schumm), Benchmark papers in Geology, pp. 283–300, Hutchinson, Ross & Dowden 1972.
- LEOPOLD, L. B., WOLMAN, M. G. & MILLER, J. P. 1964 *Fluvial Processes in Geomorphology*. W. H. Freeman, San Francisco.
- LIVERPOOL, T. B. & EDWARDS S. F. 1995 Dynamics of a meandering river. *Phys. Rev. Lett.* **75**, 3016–3019.
- MARANI, M., LANZONI, S., ZANDOLIN, D., SEMINARA, G. & RINALDO, A. 2002 Tidal meanders. *Water Resour. Res.* **38**, 1225–1239.
- MEYER-PETER, E. & MÜLLER, R. 1948 Formulas for bedload transport. *III Conf. Intl Assoc. of Hydraul. Res.*, Stockholm, Sweden.
- NANSON, G. C. & HICKIN, E. J. 1983 Channel migration and incision on the Beatton River. *J. Hydr. Engng* **109**, 327–337.
- PARKER, G. & ANDREWS, E. D. 1986 On time development of meanders bends. *J. Fluid Mech.* **162**, 139–156.
- PARKER, G., DIPLAS, P. & AKIYAMA, J. 1983 Meander bends of high amplitude. *J. Hydr. Engng ASCE* **109**, 1323–1337.
- PARKER, G. & JOHANNESSON, H. 1989 Observations on several recent theories of resonance and overdeepening in meandering channels. In *River Meandering* (ed. S. Ikeda & G. Parker) Water Res. Monograph 12, pp. 379–415. AGU.
- PIZZUTO, E. J. & MECKELNBURG, J. S. 1989 Evaluation of a linear bank erosion equation. *Water Resour. Res.* **25**, 1005–1013.
- REPETTO, R., TUBINO, M. & ZOLEZZI, G. 1999 Free bars in rivers. *J. Hydr. Res.* **37**, 759–775.
- ROZOVSKIJ, I. L. 1961 *Flow of Water in Bends of Open Channels*. Israel Program for Scientific Translations, Jerusalem, Israel.
- SEMINARA, G. & SOLARI, L. 1998 Finite amplitude bed deformations in totally and partially transporting wide channel bends. *Water Resour. Res.* **34**, 1585–1598.
- SEMINARA, G., SOLARI, L. & PARKER, G. 2003 Bed load at low Shields stress on arbitrarily sloping beds: failure of the Bagnold hypothesis. *Water Resour. Res.* **38**, 31–1/31–16.
- SEMINARA, G. & TUBINO, M. 1992 Weakly nonlinear theory of regular meanders. *J. Fluid Mech.* **244**, 257–288.
- SEMINARA, G., TUBINO, M. & ZARDI, D. 1994 Evoluzione planimetrica dei corsi d’acqua meandriiformi dall’incipiente formazione al “cut-off”. *XXIV Convegno di Idraulica e Costr. Idrauliche, Napoli, 20–22 settembre*, T4-207. (In Italian).
- SEMINARA, G., ZOLEZZI, G., TUBINO, M. & ZARDI, D. 2001 Downstream and upstream influence in river meandering. Part 2. Planimetric development. *J. Fluid Mech.* **438**, 213–230.
- SHIELDS, A. 1936 Anwendung der Ähnlichkeitsmechanik und der turbulenzforschung auf die geschiebebewegung. *Mitt. Preuss. Versuchsanst. Wasserbau Schiffbau*, 26.
- SMITH, C. E. 1998 Modeling high sinuosity meanders in a small flume. *Geomorphology* **25**, 19–30.
- SOLARI, L. & SEMINARA, G. 2005 On width variations in river meanders. *Symp. on River, Coastal and Estuarine Morphodynamics, Urbana, Illinois, 4–7 October*.
- SOLARI, L., NOBILE, G. P., BOLLA PITTALUGA, M. & SEMINARA, G. 2006 On why the river width oscillates in meandering channels. In preparation.
- STOLUM, H. 1996 River meandering as a self-organization process. *Science* **271**, 1710–1713.

- SUN, T., MEAKING, P., JOSSANG T. & SCHWARZ, K. 1996 A simulation model for meandering rivers. *Water Resour. Res.* **32**, 2937–2954.
- TUBINO, M. & SEMINARA, G. 1990 Free-forced interactions in developing meanders and suppression of free bars. *J. Fluid Mech.* **214**, 131–159.
- ZOLEZZI, G., GUALA, M., TERMINI D. & SEMINARA, G. 2005 Experimental observations of upstream overdeepening. *J. Fluid Mech.* **531**, 191–219.
- ZOLEZZI, G. & SEMINARA, G. 2001 Downstream and upstream influence in river meandering. Part 1. General theory and application to overdeepening. *J. Fluid Mech.* **438**, 183–211.